Spectrum-Map-Empowered Opportunistic Routing for Cognitive Radio Ad Hoc Networks

Shih-Chun Lin, *Student Member, IEEE*, and Kwang-Cheng Chen, *Fellow, IEEE*

***Abstract*—Cognitive radio (CR) has emerged as a key technology for enhancing spectrum efficiency by creating opportunistic transmission links. Supporting the routing function on top of opportunistic links is a must for transporting packets in a CR ad hoc network (CRAHN) consisting of cooperative relay multiradio systems. However, there lacks a thorough understanding of these highly dynamic opportunistic links and a reliable end-to-end transportation mechanism over the network. Aspiring to meet this need, with innovative establishment of the spectrum map from local sensing information, we first provide a mathematical analysis to deal with transmission delay over such opportunistic links. Benefitting from the theoretical derivations, we then propose spectrum-map-empowered opportunistic routing protocols for regular and large-scale CRAHNs with wireless fading channels, employing a cooperative networking scheme to enable multipath transmissions. Simulations confirm that our solutions enjoy significant reduction of end-to-end delay and achieve dependable communications for CRAHNs, without commonly needed feedback information from nodes in a CRAHN to significantly save the communication overhead at the same time.**

***Index Terms*—Ad hoc networks, cognitive radio (CR) networks, cooperative relay, dynamic spectrum access (DSA), multihop networks, opportunistic routing, spectrum map.**

I. Introduction

As THE FCC [1] promotes the spectrum usage of databases to regulate the use of licensed bands for unlicensed users, cognitive radio (CR) [2], which equips short-range communication and sensing capability, is being widely considered for efficient spectrum utilization. Dynamic spectrum access (DSA) allows multiple CRs to access the transmission opportunity after detecting the spectrum hole from utilization of primary system(s) (PS) [3]. Once successful DSA is achieved, the packets due to successful leverage of transmission opportunities could be transported to the destination node, which results in a demand for multihop networking of a CR ad hoc network (CRAHN) consisting of CRs and PSs via cooperative relay technology [4]–[6]. However, CRAHN routing still remains a technology challenge.

To dynamically access the preassigned spectrum bands, CR must collect and process information about co-existing users within the spectrum of interests, which requires advanced sensing and signal-processing capabilities [3], [7]. Inspired by general spectrum sensing [8], sensing information of both the CR's transmitter (CR-Tx) and the CR's receiver (CR-Rx) is critical. This suggests the construction of the spectrum map over possible routing paths. The spectrum map exhibits the available spectrum with geographic area, through sensing and locationing, and various inference techniques can be applied to construct such a spectrum map [9]–[14]. Thus, for the dynamic and the opportunistic nature of a CRAHN, the spectrum map serves as an information aggregation to maintain cumulative information in a reliable way and in a resource-efficient way. As the sporadically available link and heterogeneous nature of the CRAHN [15] induces another critical challenge in the routing algorithm design, cooperative communication emerges to support transmissions in such a highly dynamic wireless ad hoc network. Akyildiz *et al.* [16] provided a complete survey that advocates cooperative spectrum-aware communication protocols, which considers spectrum management for its cross-layer design. Characterizing the behavior and constraints for a multihop CR network from multiple layers, Hou *et al.* [17] developed a mathematical formulation to minimize the required spectrum resource for a set of user sessions. For mobile CRAHNs, Chowdhury and Felice [18] proposed a SEARCH protocol that jointly undertakes path and channel selection to avoid PSs' activity regions during route formation. Chowdhury *et al.* [19] further incorporated spectrum awareness in a transport control protocol for CRAHNs. Abbagnale and Cuomo [20] provided the Gymkhana scheme as a connectivity-based routing protocol that routes the information to avid network zones without guaranteed stable and high connectivity. Cesana *et al.* [6] presented an extensive overview for routing in CR networks with respect to available spectrum knowledge. Examining a joint problem of relay node assignment and multihop flow routing, Sharma *et al.* [21] delineated the benefits of exploiting cooperative communication in multihop wireless networks. Feng and Yang [22] analyzed the throughput of secondary networks and provided the information on how a CR channel can be utilized at the network level. Yazane *et al.* [23] focused on a three-node chain topology and provided end-to-end throughput analysis for multihop wireless networks. To leverage multiple-input multiple-output in a cooperative CR network, Hua *et al.* [24] studied cooperative forwarding with two-phase transmissions among primary and secondary

Manuscript received January 30, 2013; accepted October 29, 2013. Date of publication January 2, 2014; date of current version July 10, 2014. This work was supported by Intel, National Taiwan University, and National Science Council under Contract NSC 101-I-002-001, Contract NTU 102R7501, and Contract NSC 102-2221-E-002-016-MY2. The review of this paper was coordinated by Prof. J.-M. Chung.

S.-C. Lin was with the INTEL-NTU Connected Context Computing Center, Taipei 10617, Taiwan, and was also with the School of Electrical and Computer Engineering, Purdue University, West Lafayette, IN 47907 USA. He is now with the School of Electrical and Computer Engineering, Georgia Institute of Technology, Atlanta, GA 30332-0250 USA (e-mail: slin88@ece.gatech.edu).

K.-C. Chen is with the Graduate Institute of Communication Engineering, National Taiwan University, Taipei 10617, Taiwan (e-mail: chenkc@cc.ee.ntu.edu.tw).

Color versions of one or more of the figures in this paper are available online at http://ieeexplore.ieee.org.

Digital Object Identifier 10.1109/TVT.2013.2296597

0018-9545 © 2014 IEEE. Personal use is permitted, but republication/redistribution requires IEEE permission.
See http://www.ieee.org/publications_standards/publications/rights/index.html for more information.

systems. To establish spectrum map via cooperative sensors, Lien *et al.* [25] facilitated quality-of-service (QoS) guarantees in cyber-physical systems by proposing CR resource management. Novel opportunistic routing [26]–[29] allows assistance by intermediate nodes in a probabilistic manner to explore cooperative diversity efficiently and practically with significant throughput gain. Aiming for dynamic ad hoc networks, Cedric [26] dealt with the mobility issue through continuously modifying the packet header. Via a network coding approach, MORE [27] provides opportunistic routing for a multicasting scenario. Under Rayleigh fading channels, Zheng and Li [28] provided analytical models to characterize the performance of routings. Khalifé *et al.* [29] indicated that the proper time for opportunistic forwarding in CR networks depends on the proportional timescale of the primary bands' idle time with cognitive communication duration. It is noted that the opportunistic routing concept in [29] is close to the ideas in this paper. However, there still lacks a realistic routing algorithm for CRAHNs with realistic network size, based on theoretical mathematical analysis of data transportation with opportunistic communication links due to wireless fading, access, and operations. Furthermore, relying on feedback communication overheads from nodes can significantly reduce the spectrum efficiency, and thus, CRAHN nodes shall simply rely on sensing and inference to execute networking functions such as routing.

In this paper, aiming at networking in multihop CRAHNs, rather than only focusing on theoretical derivations or routing algorithm designs, we provide the mathematical analysis of transmission delay and propose spectrum-map-empowered opportunistic routing (SMOR) algorithms based on theoretical results. We first tackle the general CRAHNs into regular CRAHNs and large-scale CRAHNs regarding network size. Mumey *et al.* [30] only dealt with multihop networking in a mesh structure. Cacciapuoti *et al.* in [31] and Chowdhury *et al.* in [19] tried to embed location information but heavily relied on feedback from nodes to imply tremendous communication overhead. Here, without relying on the feedback information from nodes to avoid tremendous complexity, regular networks account for the networks with few nodes and well-known network topologies, whereas large-scale networks account for the network with a great number of nodes, and its topology is characterized by spatial distribution of nodes. CR's data transportation is thoroughly studied with the spectrum map idea [9], [11]–[13], [32] for both types of CRAHNs, and the transmission delay over opportunistic links is obtained by queueing network theory. This delay attribute dominates the transmission capability of forwarders for multihop networking, and thus, it plays a crucial role for reliable and effective networking. Employing such analytic results with cooperative communications, two SMOR algorithms are respectively proposed for regular and large-scale CRAHNs with wireless fading channels. These algorithms, based on both delay and possible connections to neighboring nodes, employ a cooperative networking scheme to enable multipath transmissions and facilitate reliable end-to-end transportation. We summarize our methodology as follows.

1) Being aware that the only feasible sensing information of available transmission is around the neighborhood of each node, we examine the network topology and opportunistic links with spectrum map under fading channels.
2) For regular CRAHNs, the mathematical analysis for transmission delay of multihop communications is examined via Markov chain modeling and queueing network theory, and SMOR-1 algorithm is proposed to exploit opportunistic selections for cooperative relay regarding link transmission qualities.
3) On the other hand, for large-scale CRAHNs, the corresponding delay of opportunistic links is derived via stochastic geometry and queueing network analysis, and SMOR-2 algorithm is proposed to fulfill geographic opportunistic routing, exhibiting cooperative diversity in such large-scale networks.

Simulation results confirm that our solutions enjoy less end-to-end delay due to theoretical analysis and yield dependable communications for regular and large-scale CRAHNs. Considering spectrum map together with opportunistic routing for cross-layer designs, our proposed methodology resorts to fundamental routing algorithms via analytical analysis and creates great application potential in spectrum sharing networks, such as machine-to-machine communications and wireless sensor networks.

The rest of this paper is organized as follows. The system model is presented in Section II. Mathematical analysis for data transportation in regular CRAHNs is proposed in Section III and the corresponding analysis in large-scale CRAHNs is examined in Section IV. Two routing protocols (i.e., SMOR-1 and SMOR-2 algorithms) are proposed in Section V to bring the theoretical results into practice. Performance evaluation is provided in Section VI and this paper concludes in Section VII.

II. System Model

To exploit the merit of spectrum map for routing algorithm designs, we adopted the underlay CRAHN paradigm [7] that mandates concurrent PSs' and CRs' transmissions only if the interference generated by CR-Txs at the PS's receivers (PS-Rxs) is below some acceptable threshold. That is, CR-Tx's transmit power should be limited by the interference constraint. In the following, we first present the network model regarding network topology and spectrum map usages. Then, we give four types of traffic models for both regular and large-scale CRAHNs. Important notations in this paper are summarized in Table I.

A. Network Model

According to [16], an entire CRAHN topology consists of a CR source (CR_S), a CR destination (CR_D), several CRs as the cooperative relay nodes (CR_Rs) that can forward the packet(s) from CR_S to CR_D, and primary mobile stations (PSs) with its infrastructure. CRs forward the traffic through relay nodes without PSs' help and shall prevent PSs' transmission from interruption. We assume that there are n CR nodes, exclusive CR_D in CRAHN. The ith CR node has T_i possible opportunistic paths to CR_D and the jth opportunistic path (denoted by P_{ij}) consisting of L_{ij} links. Therefore, the opportunistic paths for the ith CR node to CR_D are labeled by $P_i = \{P_{i1}, P_{i2}, \ldots, P_{iT_i}\}$.

TABLE I
USEFUL NOTATIONS IN THIS PAPER

Notation	*Description*	*Notation*	*Description*
T_i	Amounts of opportunistic paths from i^{th} CR node to CR_D	P_{ij}	The j^{th} path to CR_D from i^{th} CR node
L_{ij}	Amounts of links for j^{th} path of i^{th} CR node to CR_D	Δt_s	The period of the s^{th} time slot
λ	CR's Poisson packet arrival rate	μ	CR's packet service rate
Regular CRAHN			
N	Amounts of spectrum blocks for quantized spectrum map	N_{PS}	Amounts of spectrum blocks used by PS
l	The length of spectrum block	M_k	Amounts of blocks need for CR's the k^{th} opportunistic link
σ_{ij}	Spectrum available probability of CR_i-CR_j	ν_{ij}	Successful transmission rate of CR_i-CR_j
Large-scaled CRAHN			
ψ	PS-Rx's required power level	W_T	Total spectrum band under concern
$\lvert h_{iT-jR}\rvert^2$	The exponential distributed channel gain with parameter H_{ij} where i (j) is P for PS and S for secondary CR		
N_{iT-jR}	The noise power between node i and j where i (j) is P for PS and S for secondary CR		
τ_{PR} and τ_r	The SINR requirement for successful PSs' and CRs' link transmissions.		
$\tilde{\lambda}_{PT}$ and $\tilde{\lambda}_{ST}$	PS's and CR's densities		
P_{PT} and P_{ST}	PSs' and CRs' transmitted powers		

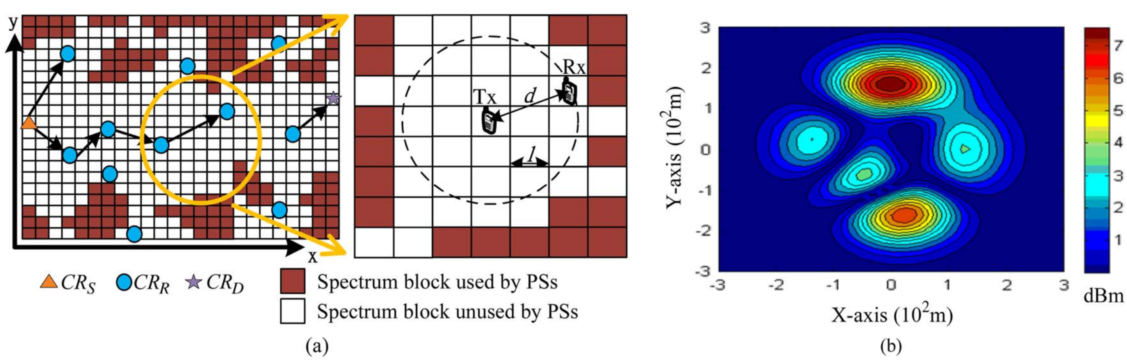

Fig. 1. Spectrum map for spectrum-aware communication in regular and large-scale CRAHNs. (a) Quantized spectrum map for a regular CRAHN. (b) Spectrum map for a large-scale CRAHN.

As mentioned, the spectrum map indicates the available spectrum with the geographic area, acting as an information aggregation platform of all kinds of sensing and inference results to serve CRAHN functions. For regular CRAHNs, we consider a quantized spectrum map as in Fig. 1(a) and query link qualities down paths for CR-Txs in Section III. On the other hand, to seek more opportunities for CRs' transmissions in large-scale CRAHNs, we study a general spectrum map as in Fig. 1(b) that reveals the actual sensing results (i.e., power detection) instead of just two states for quantized maps. In addition to the available spectrum map, CR-Tx could exercise the power level, which prevents the interference to the PS-Rx via the reciprocal inference as in Fig. 2. Specifically, due to the broadcast nature for every transmission via the same medium in wireless communication, CR-Tx might overhear the transmission from a PS-Rx's location, while PS devices are in RTS-CTS or some other control signaling period. CR-Tx then predicts the distance to the PS-Rx from the channel model for PS-Rx to CR-Tx and deploys the distance into the conversely channel model (i.e., from CR-Tx to PS-Rx) to obtain its interference to PS-Rx. Such reciprocal inference accompanied with the spectrum map is examined in Section IV. In sum, aiming for highly dynamic communication links in CRAHNs,

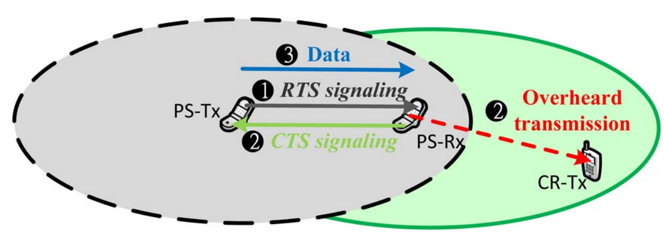

Fig. 2. Wireless overhearing phenomenon between heterogeneous CR and PS devices.

we utilize the cross-layer design to employ the broadcasting nature of wireless communication with cooperative multipath transmission.

B. Traffic Model

Four patterns of data packet transmissions are considered for both regular and large-scale CRAHNs as follows:

- deterministic packet size in slotted system (DS);
- variable packet size in slotted system (VS);
- deterministic packet size in unslotted system (DU);
- variable packet size in unslotted system (VU).

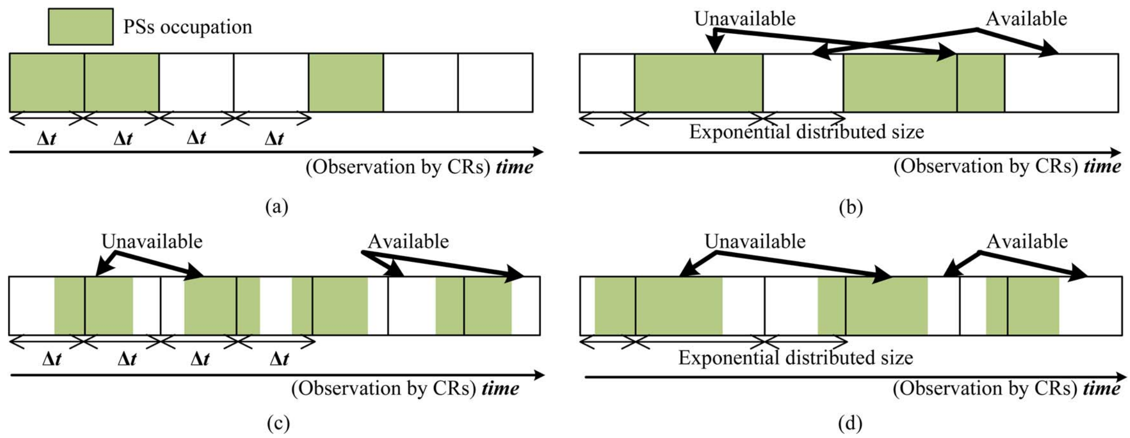

Fig. 3. Time diagrams for CRs' spectrum usages in slotted and unslotted systems. (a) Deterministic packet size for the slotted system (DS). (b) Variable packet size for the slotted system (VS). (c) Deterministic packet size for the unslotted system (DU). (d) Variable packet size for the unslotted system (VU).

The system perspective (i.e., slotted and unslotted) comes from CRs' observation, which characterizes the interaction between PSs' and CRs' traffic. For the slotted perspective in Fig. 3(a) and (b), it is supposed that CR_S and CR_D are synchronous with time slot, and the sth time slot $[t_s, t_{s+1})$ is equal to Δt_s, where $s \in \mathbb{I}$. PS's transmission activity can be modeled as an embedded two-state discrete-time Markov chain (DTMC), with state "1" represented for spectrum available and state "0" represented for spectrum unavailable when considering opportunistic link [4], [15]. In each slot (i.e., Δt_s), if PS is active/idle for transmission(s), the entire time slot is unavailable/available for CR transmission. On the other hand, for the unslotted perspective in Fig. 3(c) and (d), we adopt the traffic flow concept that CR's link utilization can be interrupted by PS's traffic. Therefore, there is one system perspective for each studied CRAHN. We further consider two types of packet sizes that are transmitted by PSs' and CRs' transmitter–receiver pairs. The deterministic packet size suggests that Δt_s is equal to Δt for all time slots. This means that in each time slot, a single packet can be transmitted for PS's or CR's traffic, assuming PS and CR have the same packet size. The variable packet size deals with the exponential distributed packet size to generalize our study. Hence, all possibly traffic patterns are thoroughly included by our four traffic patterns.

III. Regular Cognitive Radio Ad Hoc Networks

The regular CRAHN aims for the network with regular size as the required information for transmissions is likely aware for each CR. In the following, under four kinds of traffic patterns (i.e., DS, VS, DU, and VU), we examine essential characteristics (i.e., spectrum availability, wireless fading, and link service rate) for networking in the regular CRAHN and then provide the end-to-end delay for data transportation via queueing network analysis.

A. Problem Formulation for Regular CRAHN

To mitigate intersystem interference for networking in the CRAHN, CRs' link transmissions should notice PSs' spectrum usage, and we model spectrum available probability for CRs by formulating Markov chains with the spectrum map in Section III-A1. Furthermore, to accommodate the effects from the wireless communication channel, the successful transmission rate is examined in Section III-A2. The link service rate of the CR's packet for an underlay paradigm is further proposed in Section III-A3.

1) Spectrum Availability via Markov Chain Modeling: With the quantized spectrum map shown in Fig. 1(a), we assume that there are N spectrum blocks with N_{PS} used by PS. For a successful transmission over opportunistic link, the transmission should not interrupt other's traffic from the CR-Tx aspect, and it should not be disturbed by other's traffic from the CR-Rx aspect. Specifically, CR-Tx's transmitted power must not affect PSs' used spectrum blocks along the route to CR-Rx. Moreover, CR-Rx's occupied block must be unused by PSs for successful reception from CR-Tx. The length of the spectrum block (i.e., l) is suggested by the area that CR-Rx can conduct successful signal reception, even under interference. Thus, the number of blocks M_k needed to be unoccupied for CR's transmitter–receiver pair of the kth link follows $d/l \leq M_k \leq \lceil \pi d^2/l^2 \rceil$, where d is the distance between the CR's transmitter and receiver. It provides the orthogonal property between PSs' and CRs' spectrum usages in the spatial domain for the considered underlay paradigm.

As for the slotted perspective (i.e., DS and VS cases), the spectrum availability for a single spectrum block implies the probability of the block being available at sample time. For a single spectrum block, three statistics of spectrum measurement are obtained from the map as follows:

- traffic load φ;
- correlated spectrum block for PS η; and
- usage dependence for PS ξ.

φ specifies the unavailable ratio of the spectrum block and can be given according to the direct decision from the location in the map (i.e., φ is either 0 or 1) or $\varphi = N_{PS}/N$ with the assumption that a single spectrum block is picked in a uniform manner. η and ξ specify the dependence of spectrum block usage for PS. With the transition probability matrix of the spectrum block given from the given statistics and the initial state probability (denoted by ω), state probability $\omega^{(s)}$ in the sth time slot $[t_s, t_{s+1})$ is obtained by

$$[\,1-\omega^{(s)} \quad \omega^{(s)}\,] = [\,\varphi \quad 1-\varphi\,]\begin{bmatrix} \xi & 1-\xi \\ 1-\eta+\xi & \eta-\xi \end{bmatrix}^s. \quad (1)$$

Furthermore, without knowledge of the initial state probability, limiting the state probability of a single spectrum block is adopted for an irreducible ergodic Markov chains as $\omega^* = 1-\xi/2-\eta$. Therefore, the available probability of the kth opportunistic link in the sth time slot $[t_s, t_{s+1})$ under the slotted perspective (i.e., the probability that M_k spectrum blocks being unused by PSs) follows a Bernoulli process with $\sigma_{S_k^s} = \prod_{M_k}(\omega^{(s)})$ or $\prod_{M_k}(\omega^*)$, which depends on the knowledge of the initial state probability. Practically, $\sigma_{S_k^s}$ is accessible for CRs by information collection referred to as the CR network tomography [33]. Alternatively, for the unslotted perspective (i.e., DU and VU), the spectrum availability for a single spectrum block accounts for the probability of the block being available at sample time (i.e., ω_{DU} and ω_{VU}) and the probability of the residual available time being larger than the transmission time (i.e., ζ_{DU} and ζ_{VU}). Thus, the available probability of the kth opportunistic link under the unslotted perspective follows a Bernoulli process with $\sigma_{DU_k} = \prod_{M_k}(\omega_{DU}\zeta_{DU})$ for deterministic packet size or with $\sigma_{VU_k} = \prod_{M_k}(\omega_{VU}\zeta_{VU})$ for variable size.

2) Wireless Channel Fading: Each attempt to transmit a packet of the kth link of the P_{ij} path for the ith CR's transmission is modeled as a Bernoulli process with a successful transmission rate ν_k (i.e., the opposite of outage probability for the received signal-to-noise ratio (SNR) SNR_r lower than the threshold κ). For path-loss and shadowing environment, the received power at given distance from the transmitter is lognormally distributed [34] and $\nu_k = 1 - Q([P_{\min} - P_s - 10\log_{10} K + 10\alpha\log_{10}(d/d_0)]/\sigma_{\beta_{dB}})$, where P_s is transmitted signal power, and $P_{\min}$ is a target minimum received power level. d_0 is a reference distance for antenna far field, and d is the distance between the transmitter and the receiver. K is an unitless constant that depends on the antenna characteristics and the average channel attenuation. α is the path-loss exponent and β is the shadowing effect parameter and is modeled as lognormal distribution with mean 0 dB and standard derivation σ_β dB. In addition, as for the multipath case, received signal may suffer from Rayleigh fading and $\nu_k = 1 - \exp(-\kappa N_0 d^\alpha/\Omega P_s d_0^\alpha)$.

3) Link Service Rate for Underlay Paradigm: In Fig. 3, CRs' transmission should be developed regarding traffic patterns, which involve the service time (or rate) of opportunistic links. With regard to deterministic packet size, the service time is fixed and is equal to Δt for each CRs' packet transmission. On the other hand, for variable packet size, different fundamental wireless fading channels [35] (e.g., lognormally distributed model for large-scale fading, Rayleigh fading for small-scale fading, and the fast-fading model) are considered to obtain the service rate as follows. Given link's capacity C, total concerned band W_T, and PS's activity τ $(0 \le \eta \le \tau \le 1)$, the service rate of opportunistic link under the fading channel is given by

$$\mu = B\eta W_T E\left[\log_2\left(1+\frac{|h|^2(d/d_0)^{-\alpha}P_s}{N_0}\right)\right]$$
$$= \begin{cases} B\eta W_T \log_2\left(1+\frac{K(d/d_0)^{-\alpha}10^{\beta/10}P_s}{N_0}\right) \\ \text{in large scale fading} \\ B\eta W_T \log_2\left(1+\frac{|h|^2(d/d_0)^{-\alpha}P_s}{N_0}\right) \\ \text{in Rayleigh fading} \\ B\eta W_T \frac{(d/d_0)^{-\alpha}P_s\sqrt{\pi\Omega}}{2N_0}\log_2(e) \\ \text{in fast fading with low SNR} \\ B\eta W_T\left[\ln\left(\frac{(d/d_0)^{-\alpha}P_s}{N_0}\right)+E\left[\ln\left(|h|^2\right)\right]\right]\log_2(e) \\ \text{in fast fading with high SNR} \end{cases} \quad (2)$$

where B denotes packet per bit. With these essential elements of CRs' opportunistic links, we are in place for the end-to-end delay in regular CRAHNs as follows.

B. Queueing Network Analysis

While CRs' traffic might be interrupted by PSs' traffic, end-to-end delay regarding CR's link access delay accounts for reliable communications. In the following, via queueing network analysis [36], we first model an opportunistic link as a queue with additional access delay. Then, we study opportunistic link delay and opportunistic path delay under a specific traffic pattern for regular CRAHNs.

1) Queue Models for Various Traffic Patterns: According to Section II-B, we model the kth opportunistic link of the P_{ij} path for the ith CR node within four cases. Poisson distribution is chosen as the traffic arrival rate (i.e., packets arrive according to a Poisson process), since it is generally considered as a good model for the aggregate traffic of a large number of similar and independent packet transmissions [37]. For deterministic packet size (i.e., all packets have equal length), every transmitted packet is periodically served. Alternatively, exponential distribution is chosen for variable packet size due to its memoryless character [37]. In the sth time slot $[t_s, t_{s+1})$ of the slotted system, λ_k^s denotes the CR's Poisson packet arrival rate, and $E[S_k^s]$ denotes the packet service rate with service time S_k^s. For the unslotted system, λ_{CR}^k denotes the CR's Poisson packet arrival rate, and μ_{CR}^k denotes the packet service rate with service time S_{CR}^k. λ_{PS}^k denotes the PS's Poisson packet arrival rate, and μ_{PS}^k denotes the packet service rate with service time S_{PS}^k. To simplify notations, we do not specify the kth link and the sth time slot and use $\lambda_{CR} = \lambda$ in the following derivations.

- Deterministic Packet Size in Slotted or Unslotted System (DS or DU): We model the opportunistic link as $M/D/1/\infty/FCFS$ queue. In Section III-A2, a wireless fading channel can be treated as an erasure channel and suffers packet loss. Therefore, each attempt to transmit a packet is a Bernoulli process with successful transmission rate ν. For slotted systems, assuming $Y \sim Geo(\nu)$ accounts for a successful transmission rate and $X \sim Geo(\sigma)$ accounts for available probability from opportunistic nature (where Geo stands for geometric distribution), X and Y are uncorrelated from independent events, and total service time S of the queue model becomes the summation from X_1 to X_Y. Thus, we model $M/Geo/1/\infty/FCFS$ with $Geo(c_S)$, where c_S is equal to $\sigma\nu$. As for unslotted systems, the successful transmission rate for PSs' or CRs' traffic is ν_{PS} or ν, respectively. The spectrum availability is a Bernoulli process with probability $\sigma_{DU} = \prod_{M_k}(\omega_{DU}\zeta_{DU})$. ω_{DU} is the probability of a channel being available for transmission at the observation time, and $\omega_{DU} = 1 - \lambda_{PS}\Delta t/\nu_{PS}$. ζ_{DU} is the probability of the residual available time being larger than the transmission time as $\zeta_{DU} = 1 - \sum_{k=1}^{\infty}[(1-\exp^{-\lambda_{PS}\Delta tk})\nu(1-\nu)^{k-1}] = \nu\exp^{-\lambda_{PS}\Delta t}/(1-\exp^{-\lambda_{PS}\Delta t} + \nu\exp^{-\lambda_{PS}\Delta t})$. Therefore, we adopt the $M/Geo/1/\infty/FCFS$ queue model with $Geo(c_{DU})$, where c_{DU} is equal to $\sigma_{DU}\nu$.

- Variable Packet Size in Slotted or Unslotted System (VS or VU): We model such an opportunistic link as $M/M/1/\infty/FCFS$ queue. ν still represents the successful transmission rate. For exponential service rate μ and Bernoulli process with available probability σ, the equivalent service rate is $\mu\sigma$ by the formulation of geometrical sum of exponential distribution. We have $M/M/1/\infty/FCFS$ queue with service rate μc_S for the slotted case. In unslotted systems, spectrum availability follows a Bernoulli process with $\sigma_{VU} = \prod_{M_k}(\omega_{VU}\zeta_{VU})$ where $\omega_{VU} = 1 - \lambda_{PS}/\mu_{PS}$ and $\zeta_{VU} = \mu_{CR}/(\lambda_{PS} + \mu_{CR})$. Thus, we have the $M/M/1/\infty/FCFS$ queue model with service rate μc_{VU}, where c_{VU} is equal to $\sigma_{VU}\nu$.

2) Opportunistic Link Delay: In the unslotted perspective, CR's traffic can be intervened by PS's traffic even in an available slot of CR's transmission. The CR's traffic arrival rate is λ under successful transmission rate ν, and the PS's traffic arrival rate is λ_{PS}. For deterministic packet size, the available probability for CR's traffic is σ_{DU}, and the successful transmission rate of PS's traffic is ν_{PS}. For variable packet size, the CR's traffic service rate is μ with available probability σ_{VU}, and the PS's traffic service rate is μ_{PS}. The link delay for various traffic patterns is obtained in the following.

Lemma 1: Given CR's traffic rate λ no more than the service rate $1/E[S]$, the opportunistic link delay for the DU or VU case is (3) or (4), respectively. Alternatively, the opportunistic link delay for the DS or VS case is (5) or (6), respectively.

Proof: To avoid the buffer size becoming infinity, the packet arrival rate of λ should be less than or equal to the packet service rate $1/E[S]$ for service time S. With deterministic packet size, $E[S] = \Delta t/c_{DU}$ and $E[S^2] = \Delta t^2(2 - c_{DU})/c_{DU}^2$. By the *Pollaczek–Khinchin* (P-K) formula [36], the expected waiting time of a packet in queue is shown by $W_q = \lambda E[S^2]/2(1 - \lambda E[S]) = \lambda\Delta t^2(2 - c_{DU})/2c_{DU}(c_{DU} - \lambda\Delta t)$. The delay for the DU case is

$$\frac{\Delta t(2-\lambda\Delta t)}{2(c_{DU}-\lambda\Delta t)}. \tag{3}$$

With variable packet size, the waiting time distribution is $w(t) = (\mu c_{VU} - \lambda)\exp^{-(\mu c_{VU}-\lambda)t}$ for $t > 0$ and $W_q = \lambda/\mu c_{VU}(\mu c_{VU} - \lambda)$. The delay for opportunistic link within the VU case is

$$\frac{1}{\mu c_{VU}} + W_q = \frac{1}{\mu c_{VU} - \lambda}. \tag{4}$$

From above, for the DS case

$$\frac{\Delta t(2-\lambda\Delta t)}{2(c_S-\lambda\Delta t)} \tag{5}$$

or for the VS case

$$\frac{1}{\mu c_S - \lambda}. \tag{6}$$

■

3) Opportunistic Path Delay: Since one-hop opportunistic paths as direct links are provided in Section III-B2, we derive the multihop path delay by first considering two-hop opportunistic paths and then extending to N-hop opportunistic paths. It is noted that to derive path delay for a multihop opportunistic path, we consider single-path transmission as such single chain link assumption simplifies the calculations for metrics and are well fitted for a highly dynamic CRAHN, without loss of generality.

Lemma 2: Given CR's traffic arrival rate λ to be no more than the lower service rate (i.e., $\min_{1\le j\le 2} 1/E[S_j]$), the path delay of a two-hop opportunistic path for the DU or VU case is (7) or (8), respectively. Alternatively, the one for the DS or VS case is (9) or (10), respectively.

Proof: To avoid the buffer size becoming infinity, the packet arrival rate of λ should be less than or equal to the lower service rate of two hops. That is, $\lambda \le \min_{1\le j\le 2} 1/E[S_j]$. The path delay can be derived from a tandem queue model by summation of waiting time random variables for each single hop. With deterministic packet size, from **Lemma 1**, we have $E[S_1] + \lambda E[S_1^2]/2(1 - \lambda E[S_1])$ as the mean delay of the first hop. Since Poisson arrival with rate λ to the path can be approximated as a Bernoulli process with probability q, the Bernoulli process is further modeled as two-state DTMC with transition probabilities $a_{01}^{(0)}$ and $a_{10}^{(0)}$, and thus, $q = a_{01}^{(0)}/(a_{10}^{(0)} + a_{01}^{(0)})$. $a_{01}^{(0)}$ is equal to λ, and the sum of $a_{01}^{(0)}$ and $a_{10}^{(0)}$ is equal to 1. Then, with $GI/Geo/1$ queue modeling [38], the output process of the first hop is approximated as an on–off process with transition probabilities $a_{11}^{(1)}$ and $a_{01}^{(1)}$, both being equal to λ as $a_{11}^{(1)} = 1/E[S_1] - a_{01}^{(0)}(1-\rho_1)/\rho_1 = \lambda$ and $a_{01}^{(1)} = \lambda(1 - a_{11}^{(1)})/(1 - \lambda) = \lambda$. We get the mean delay of the second hop with ρ_2 for the server utilization: $E[w_2] = 1 + \rho_2(1-\mu_2)/a_{01}^{(1)}(1 - \rho_2) = 1 + (E[S_2] - 1e)/(1 - \lambda E[S_2])$. Therefore, two-hop opportunistic path delay for the DU case is

$$\left(\frac{\Delta t(2-\lambda\Delta t)}{2(c_{DU}-\lambda\Delta t)}\right) + \left(1 + \frac{E[S_2]-1}{1-\lambda E[S_2]}\right). \tag{7}$$

For the VU case, w_1 is the waiting time of the first hop with probability density function $f_{w_1}(t) = (\mu_1 c_{VU_1} - \lambda_1)\exp^{-(\mu_1 c_{VU_1}-\lambda_1)t}$, and $f_{w_2}(t) = (\mu_2 c_{VU_2} - \lambda_2)\exp^{-(\mu_2 c_{VU_2}-\lambda_2)t}$ is for the second hop, having c_{VU_i} equal to $\sigma_{VU_i}\nu_i$. The arrival rate for each link is the same as that in Burke's theorem [36] (i.e., λ_1 and λ_2 are equal to λ). Then, the delay is obtained as

$$E[w_1 + w_2] = \frac{1}{\mu_1 c_{VU1} - \lambda} + \frac{1}{\mu_2 c_{VU2} - \lambda}. \tag{8}$$

It follows from unslotted cases, for the DS or VS case, the path delay is, respectively

$$\left(\frac{\Delta t(2-\lambda\Delta t)}{2(c_S - \lambda\Delta t)}\right) + \left(1 + \frac{E[S_2]-1}{1-\lambda E[S_2]}\right) \tag{9}$$

or

$$\frac{1}{\mu_1 c_{S1} - \lambda} + \frac{1}{\mu_2 c_{S2} - \lambda}. \tag{10}$$

■

We then derive path delay of N-hop opportunistic paths for unslotted/slotted systems.

Lemma 3: Given CR's traffic arrival rate λ to be no more than the lowest service rate (i.e., $\min_{1\leq j\leq N} 1/E[S_j]$), the path delay of N-hop opportunistic path for the DU or VU traffic case is (11) or (12), respectively. Alternatively, the path delay for the DS or VS case is (13) or (14), respectively.

Proof: To avoid the buffer size becoming infinity, the packet arrival rate of λ should be less than or equal to the lowest service rate of N hops. That is, $\lambda \leq \min_{1\leq j\leq N} 1/E[S_j]$. From **Lemma 2**, since the departure process of the second hop is observed as another on–off process with transition probability $a_{01}^{(2)}$ and $a_{10}^{(2)}$, the same procedure can be applied for the N-hop path by iteratively calculating $(a_{01}^{(i+1)}, a_{10}^{(i+1)})$ from $(a_{01}^{(i)}, a_{10}^{(i)})$. Owing to the Poisson arrival process of the first hop, the output process of the $(i+1)$th hop is approximated as an on–off process with transition probabilities $a_{10}^{(i+1)}$ and $a_{01}^{(i+1)}$ being equal to λ. We have the mean delay of the $(i+2)$th hop as $E[w_{i+2}] = 1 + (E[S_{i+2}]-1)/(1-\lambda E[S_{i+2}])$. Therefore, N-hop opportunistic path delay for the DU case is

$$\left(\frac{\Delta t(2-\lambda\Delta t)}{2(c_{DU} - \lambda\Delta t)}\right) + \sum_{i=0}^{N-2}\left(1 + \frac{E[S_{i+2}]-1}{1-\lambda E[S_{i+2}]}\right). \tag{11}$$

For the VU case, N-hop opportunistic path delay is directly obtained as

$$E[w_1 + \cdots + w_N] = \sum_{i=1}^{N} \frac{1}{\mu_i c_{VUi} - \lambda}. \tag{12}$$

For the DS or VS case, the path delay is, respectively

$$\left(\frac{\Delta t(2-\lambda\Delta t)}{2(c_S - \lambda\Delta t)}\right) + \sum_{i=0}^{N-2}\left(1 + \frac{E[S_{i+2}]-1}{1-\lambda E[S_{i+2}]}\right) \tag{13}$$

or

$$\sum_{i=1}^{N} \frac{1}{\mu_i c_{Si} - \lambda}. \tag{14}$$

■

The given derivations exhibit the necessary delay for packet transmissions through a single path between CR's source–destination pair, thus playing the essential role in routing algorithms, as illustrated later in Section V.

IV. Large-Scale Cognitive Radio Ad Hoc Networks

Large-scale CRAHNs aim for the network with large size (e.g., thousands or millions of nodes), and such network can be characterized by spatial distribution of nodes [39]. Inspired by the work in [40] with regard to four kinds of node deployment scenarios (i.e., protocol model of primary interference, protocol model of n interferences, physical model, and per-node-based model), we study essential elements (i.e., power control and radio resource allocation) for networking in a large-scale CRAHN and then examine one-hop forwarding capability of CR relay via stochastic geometry analysis as follows.

A. Problem Formulation for Large-Scale Networks

To seek more transmission opportunities for spatial reuse in a more reliable way for large-scale CRAHNs, we mitigate the restriction to CRs' transmissions (i.e., allows CRs operating when the interference to PSs is below a given threshold) via power control procedures with the reciprocal inference and the spectrum map [see Fig. 1(b)] in Section IV-A1. Moveover, the link service rate of the CR's packet for such large networks is proposed by radio resource allocation in Section IV-A2.

1) Power Control Procedures: To achieve an underlay paradigm within large-scale CRAHNs, CRs' transmissions are guided by power control procedures with two steps as follows:

1) examine the maximum power that CR-Tx can apply (without avoiding PS's transmission) from the reciprocal inference;
2) characterize CR-Rx's signal-to-interference-plus-noise ratio (SINR) by the spectrum map.

The wireless overheard transmissions and wireless channel modeling are utilized for the reciprocal inference as in Fig. 2. Specifically, with these transmissions and PS devices' transmitted power (i.e., P_{PT} in the following), CR-Tx predicts the distance between CR-Tx and PS-Rx by the channel model, since the receiving strengths now only depend on the distances. We consider these procedures for four different deployment scenarios (i.e., protocol model of one primary or n interference(s), physical model, and per-node-based model) to generalize our study. Protocol models at the MAC layer seek the interferers (i.e., interference sources) within a fixed region. Furthermore, the physical model deals with the receiver SINR, which accumulates the effects from all interferers by physical-layer information (i.e., location). The avoidance region is not fixed anymore and might depend on node density. The per-node-based model proposes the effective distance extracted from the given map and does not need location information anymore. It provides each specific transmitter with dedicated power control in a distributed manner, certifying its practicability. It is noted that to increase readability, we adopt "theoretical modeling" for the protocol and physical models, considering their theoretical settings, and "engineering modeling" for the per-node-based model, considering its feasibility in engineering.

For theoretical modeling, the channel gains of wireless fading follow the exponential distributions; engineering modeling adopts the path-loss model for wireless transmissions. Thus, without precise knowledge of PS-Rx's location, CR-Tx is capable of determining the interference caused to PS-Rx(s). On the other hand, the nice feature of the spectrum map is to act as a spectrum information aggregation platform to tackle the heterogeneous nature of CR and PS devices. Enhanced by the spectrum map, CR-Tx can obtain the information about the receiving capability of CR-Rxs and, therefore, make successful transmissions to desired CR-Rxs.

2) Link Service Rate From Radio Resource Allocation: Regarding various traffic patterns (i.e., DS, VS, DU, and VU) between CRs' and PSs' as shown in Fig. 3, we shall consider radio resource allocation for the service process of opportunistic links after power control procedures. For theoretical modeling, the outage probability is q_T, and the equivalent service rate of opportunistic link with capacity C for CR's packet is $\tilde{\mu}_T = q_T BC$, where B stands for packet per bit and depends on packet size. For engineering modeling, q_P is used for the geometric service rate in deterministic packet size, and the equivalent service rate becomes $\tilde{\mu}_P = BW \log_2(1 + SINR)$ from the Shannon formula. For unslotted systems, different from the cases in regular CRAHNs that adopt available probability to characterize the opportunistic nature, actual PS's arrival traffic is precisely concerned in large-scale CRAHNs. That is, CR's link transmission can be interrupted by PS's traffic anytime (i.e., CR should avoid transmission whenever PS has its own traffic to transmit). For such kind of link transmissions, non-preemptive priority queue [36] is adopted, while PS's traffic is Poisson arrival with rate λ_{PS}, and its service rate is q_{PS} for deterministic packet size and μ_{PS} for variable one. With the crucial elements of CRs' opportunistic links, we are ready for the link transmission delay that exhibits one-hop forwarding capability of CR relay over large-scale CRAHNs in the following.

B. Stochastic Geometry Analysis

To tackle large-scale CRAHNs with regard to possible interruptions from PSs' traffic, CR's link access delay is considered via stochastic geometry analysis [39], [41] in the following. Specifically, for theoretical and engineering models in slotted/unslotted systems, we first derive the outage probability (i.e., q_T and q_P) and obtain the average service rate (i.e., $\tilde{\mu}_T$ and $\tilde{\mu}_P$). Then, we examine opportunistic link delay for such CRAHNs.

1) Protocol Model of One Primary Interference: One primary interferer exists for both PS-Rxs and CR-Rxs. The channel gain $|h_{iT-jR}|^2$ of wireless fading is modeled as exponential distribution with parameter H_{ij}, where $i(j)$ is P for PS and S for secondary CR. It involves two steps to decide the q_T for a CR's transmitter–receiver pair. We first decide the optimal transmission power P^*_{ST} for CR-Tx from PS-Rx's SINR requirement τ_{PR}. Given the probability q_o that CR-Tx overhears PS-Rx's transmission and the SINR requirement τ_r for successful CRs' link transmissions, $d_{PR-ST} = [H_{PS}\tau_r N_{PR-ST}/P_{PT} \ln(1/q_o)]^{-1/\alpha}$, where α is the path-loss exponent. With the outage probability requirement for PS-Rx ε, the successful transmission probability becomes

$$\exp\left(-\frac{H_{PP}\tau_{PR}N_{PT-PR}}{P_{PT}d_{PT-PR}^{-\alpha}}\right) \times \frac{H_{SP}P_{PT}d_{PT-PR}^{-\alpha}}{H_{SP}P_{PT}d_{PT-PR}^{-\alpha} + H_{PP}\tau_{PR}P_{ST}d_{ST-PR}^{-\alpha}} \quad (15)$$

$$P_{ST} = \frac{H_{SP}P_{PT}d_{PT-PR}^{-\alpha}}{H_{PP}\tau_{PR}d_{ST-PR}^{-\alpha}(1-\varepsilon)} \times \exp\left(-\frac{H_{PP}\tau_{PR}N_{PT-PR}}{P_{PT}d_{PT-PR}^{-\alpha}} - 1 + \varepsilon\right) \quad (16)$$

where d_{ST-PR} is measured from overheard transmission. Therefore, $P^*_{ST} = \min_{PR} P_{ST}$ and the optimal PR^* would be closest to the CR-Tx. Next, from P^*_{ST} and the interferer of CR-Rx (i.e., PS-Tx), we get q_T. The interferer is the PS-Tx that affects target CR-Rx the most and is likely closest (in effective metric) to the CR-Rx. With τ_{CR}, we have

$$q_T = \exp\left(-\frac{H_{SS}\tau_{CR}N_{ST-SR}}{P_{ST}d_{ST-PR}^{-\alpha}}\right) \times \frac{H_{PS}P_{ST}d_{ST-PR}^{-\alpha}}{H_{PS}P_{ST}d_{ST-PR}^{-\alpha} + H_{SS}\tau_{CR}P_{PT}d_{PT-SR}^{-\alpha}}. \quad (17)$$

2) Protocol Model of n Interferences: There are n interferers for PS-Rxs and CR-Rxs, given ε and τ_{PR}, the successful transmission probability is

$$\exp\left(-\frac{H_{PP}\tau_{PR}N_{PT-PR}}{P_{PT}d_{PT-PR}^{-\alpha}}\right) \times \prod_i \frac{H_{SP_i}P_{PT}d_{PT-PR}^{-\alpha}}{H_{SP_i}P_{PT}d_{PT-PR}^{-\alpha} + H_{PP}\tau_{PR}P_{ST_i}d_{ST_i-PR}^{-\alpha}}. \quad (18)$$

We then obtain P^*_{ST}. Given τ_{CR}, we have

$$q_T = \exp\left(-\frac{H_{SS}\tau_{CR}N_{ST-SR}}{P^*_{ST}d_{ST-PR}^{-\alpha}}\right) \times \prod_j \frac{H_{PS_j}P^*_{ST}d_{ST-PR}^{-\alpha}}{H_{PS_j}P^*_{ST}d_{ST-PR}^{-\alpha} + H_{SS}\tau_{CR}P_{PT_j}d_{PT_j-SR}^{-\alpha}} \quad (19)$$

where d_{ST-PR} is obtained from overheard transmission.

3) Physical Model: It is assumed that the spatial distributions of interferers follow homogeneous Poisson point processes [41] with density $\tilde{\lambda}_{ST}$ for PS-Rx and with density $\tilde{\lambda}_{PT}$ for CR-Rx, where Φ_{ST} and Φ_{PT} denote the locations. The interference for PS-Rx is $I_S = I_{ST^\dagger} + I_{ST} = P_{ST^\dagger}|h_{ST^\dagger-PR}|^2 (d_{ST^\dagger-PR})^{-\alpha} + \sum_{i\in\Phi_{ST}} P_{ST}|h_{ST_i-PR}|^2(d_{ST_i-PR})^{-\alpha}$, where $ST^\dagger$ is the CR-Tx of interests. For given ε and τ_{PR}, the successful transmission probability changes into

$$\exp\left(-\frac{H_{PP}\tau_{PR}N_{PT-PR}}{P_{PT}d_{PT-PR}^{-\alpha}}\right) \times \exp\left(-\frac{\tilde{\lambda}_{ST}H_{PP}^{2/\alpha}\tau_{PR}^{2/\alpha}P_{ST}^{2/\alpha}d_{PT-PR}^{2}K_\alpha}{P_{PT}^{2/\alpha}}\right) \times \frac{H_{ST^\dagger P}P_{PT}d_{PT-PR}^{-\alpha}}{H_{ST^\dagger P}P_{PT}d_{PT-PR}^{-\alpha} + H_{PP}\tau_{PR}P_{ST^\dagger}d_{ST^\dagger-PR}^{-\alpha}} \quad (20)$$

where $K_\alpha = 2\pi^2/\alpha \sin(2\pi/\alpha)$. Then, P^*_{ST} is obtained. The interference of CR-Rx is $I_P = \sum_{j\in\Phi_{PT}} P_{PT_j}|h_{PT_i-SR}|^2 (d_{PT_i-SR})^{-\alpha}$. With τ_{CR}, we have

$$q_T = \exp\left(-\frac{H_{SS}\tau_{CR}N_{ST-SR}}{P^*_{ST}d^{-\alpha}_{ST-PR}}\right) \times \exp\left(-\frac{\tilde{\lambda}_{PT}H^{2/\alpha}_{SS}\tau^{2/\alpha}_{CR}P^{2/\alpha}_{PT}d^2_{ST-PR}K_\alpha}{P^{*2/\alpha}_{ST}}\right) \quad (21)$$

and d_{ST-PR} is from overheard transmission.

4) Per-Node-Based Model: Due to signal propagation in fading channels, the observed spectrum map is reconstructed based on the "effective distance" for the geographic area instead of the Euclidean distance. With the power level of transmitter P_{Tx}, the power at receiver P_{Rx}, and the interferences from other transmitters being neglected (i.e., far away from the target receiver) in the spectrum map, the effective distance is $d_{eff} = (P_{Rx}/P_{Tx})^{-1/\alpha}$. Transferring the original map into an effective distance between the transmitter–receiver pair, we easily get the essential location information and exploit the power control in the per-node-based model.

For the power level ψ_r of overheard transmission from the PS-Rx, $d_{PR-ST} = (\psi_r/P_{PT})^{-1/\alpha}$. We also assume that PS-Rx's required power level is ψ, its permissible interference level is χ, and CR-Tx's maximum power is $P^{\max}_{CT}$. For the successful reception of PS-Rx from PS-Tx, the prohibited transmission region for CR-Tx under the effective distance is a disk centered at PS-Rx with radius $r_1 = (\psi/P_{PT})^{-1/\alpha}$. The full-power region (i.e., $P^{\max}_{CT}$) for CR-Tx is also a disk centered at PS-Rx with radius $r_2 = (\chi/P^{\max}_{CT})^{-1/\alpha}$. Hence, CR-Tx's maximum power function is

$$Q(r) = \begin{cases} 0 & 0 \le r \le r_1 \\ \chi(r-r_1)^\alpha & r_1 \le r \le r_2 \\ P^{\max}_{CT} & r_2 \le r \le \infty \end{cases} \quad (22)$$

where r is the distance from the PS-Rx. With d_{ST-PR} from overheard transmission, CR-Rx's SINR is

$$SINR_{CR-Rx} = \frac{d^{-\alpha}_{ST-SR}Q(d_{ST-PR})}{N+\gamma} \quad (23)$$

with the interference level at CR-Rx γ read directly from the map, and $\tilde{\mu}_P$ is further obtained through radio resource allocation. With τ_{CR}, we have

$$q_P = \begin{cases} 0 & 0 \le SINR_{CR-Rx} \le \tau_{CR} \\ 1 & \tau_{CR} \le SINR_{CR-Rx}. \end{cases} \quad (24)$$

The CR-Rx's avoidance region with interference level χ_1 is a disk centered at PS-Tx with radius $r_a = (\chi_1/P_{PT})^{-1/\alpha}$.

5) Opportunistic Link Delay for Various Deployment Scenarios: For theoretical modeling (i.e., including Section IV-B1–B3) and engineering modeling (i.e., Section IV-B4), the opportunistic link delay for the slotted system is in **Lemma 4**, and the opportunistic link delay for the unslotted system is in **Lemma 5** as follows.

Lemma 4: Given CR's traffic arrival rate λ to be no more than the service rate $1/E[S]$, for the DS traffic case, the opportunistic link delay for theoretical or engineering modeling is, respectively

$$\frac{\Delta t(2-\lambda\Delta t)}{2(q_T-\lambda\Delta t)} \quad \text{or} \quad \frac{\Delta t(2-\lambda\Delta t)}{2(q_P-\lambda\Delta t)} \quad (25)$$

for the VS traffic case, the opportunistic link delay for theoretical or engineering modeling is, respectively

$$\frac{1}{(\tilde{\mu}_T-\lambda)} \quad \text{or} \quad \frac{1}{(\tilde{\mu}_P-\lambda)}. \quad (26)$$

Proof: Follows from **Lemma 1**. ■

Lemma 5: Given CR's traffic arrival rate λ to be no more than the service rates $1/E[S_{CR}]$ and $1/E[S_{PS}]$, for the DU case, the opportunistic link delay for theoretical or engineering modeling is, respectively, (27) or (28); for the VU case, the opportunistic link delay for theoretical or engineering modeling is, respectively, (29) or (30).

Proof: To avoid the buffer size of nonpreemptive priority queue [36] becoming infinity for unslotted systems, the packet arrival rate of λ should be less than or equal to the lower service rate of CR and PS. That is, $\lambda \le \min(1/E[S_{CR}], 1/E[S_{PS}])$. With deterministic packet size, $E[S_{PS}] = \Delta t/q_{PS}$, $E[S_{CR}] = \Delta t/q_T$ for theoretical modeling, and $E[S_{CR}] = \Delta t/q_P$ for engineering modeling. Therefore, the opportunistic link delay for theoretical or engineering modeling is, respectively

$$E[S_{CR}] + \frac{\lambda_{PS}\left(E[S_{PS}]\right)^2(2-q_{PS}) + \lambda\left(E[S_{CR}]\right)^2(2-q_T)}{2\left(1-\lambda_{PS}E[S_{PS}]\right)\left(1-\lambda_{PS}E[S_{PS}]-\lambda E[S_{CR}]\right)} \quad (27)$$

or

$$E[S_{CR}] + \frac{\lambda_{PS}\left(E[S_{PS}]\right)^2(2-q_{PS}) + \lambda\left(E[S_{CR}]\right)^2(2-q_P)}{2\left(1-\lambda_{PS}E[S_{PS}]\right)\left(1-\lambda_{PS}E[S_{PS}]-\lambda E[S_{CR}]\right)}. \quad (28)$$

Alternatively, with variable packet size, the opportunistic link delay for theoretical or engineering modeling is, respectively

$$\frac{1}{\tilde{\mu}_T} + \frac{\lambda_{PS}(\tilde{\mu}_T)^2 + \lambda(\mu_{PS})^2}{\tilde{\mu}_T(\mu_{PS}-\lambda_{PS})(\mu_{PS}\tilde{\mu}_T - \lambda_{PS}\tilde{\mu}_T - \lambda\mu_{PS})} \quad (29)$$

or

$$\frac{1}{\tilde{\mu}_P} + \frac{\lambda_{PS}(\tilde{\mu}_P)^2 + \lambda(\mu_{PS})^2}{\tilde{\mu}_P(\mu_{PS}-\lambda_{PS})(\mu_{PS}\tilde{\mu}_P - \lambda_{PS}\tilde{\mu}_P - \lambda\mu_{PS})}. \quad (30)$$

■

With regard to different node deployments, the above investigations provide the one-hop forwarding capability of CR relay in terms of required forwarding time (i.e., delay), facilitating the relay section for networking in large-scale CRAHNs, as shown in Section V.

V. Protocol Description for Cognitive Radio Ad Hoc Networks

To bring analytical derivations for regular and large-scale CRAHNs into practice, we develop two routing algorithms suitable for our previous considerations. Specifically, these algorithms need to be aware of PSs' spectrum usages to avoid interference. Furthermore, getting inspiration from cooperative diversity of CR relay, it is beneficial to exploit cooperative communications in CRAHN's multihop transportation. In the following, SMOR-1 (i.e., for regular networks) and SMOR-2 (i.e., for large-scale networks) are proposed to incorporate spectrum sharing and opportunistic routing [27], [42] into routing protocol design for CRAHNs.

A. SMOR-1

Algorithm 1 (SMOR-1)

1) *Source* partitions its traffic into batches of packets for transmissions.
2) At each *Source*s available time slot, *Source* collects link information (i.e., $\delta_{i,j}$ and $\nu_{i,j}$, i, $j \in \{CR_S, n, CR_D\}$) from the map to prioritize forwarders into the candidate list regarding node metric m_i, $i \in n$, randomly mixes packets in a batch via random network coding [43], and broadcasts coded packet with the list.
3) While the ACK message is not heard from *Destination*,
   a) *Source* repeats Step 2 until it hears ACK.
   b) For each relay node z, if z receives a packet from node y, it decodes the packet, saves unheard information in its buffer, and checks the list.
      i) If z lines before y in the list, z advances its counter by its triggering ratio Φ_z.
   c) At each z's available time slot, z examines whether its counter is positive.
      i) If so, z randomly mixes its buffered packets, broadcasts coded packet with the list, and decrements its counter by one.
4) *Destination* continuously decodes the collection of coded packets to verify whether it gets all packets of the batch. If so, *Destination* broadcasts ACK back to *Source*, eliminating the packets buffered in relay nodes and enabling the next transmission batch.

The scheme exploits opportunistic relay selection regarding transmission qualities of cooperative links into packet delay. Specifically, it designs triggering ratios with counters and proposes node metrics and candidate lists in delay perspective. To establish the candidate list for *Source*, the node metric is provided in **Proposition 1**.

Proposition 1 (Node Metric m_i for Node i): For node $i \in n$, it has T_i possible opportunistic paths to CR_D and can be distinguished into a direct link, $T_i^{(2)}$ two-hop paths, up to $T_i^{(N)}$ N-hop paths, where N is the largest amount of opportunistic links (constitute opportunistic paths). Then, node metric m_i is obtained as the minimum path delay of these T_i paths.

It is noted that the required path delay is stated in **Lemmas 1–3**. Furthermore, we formulate the CR node metric as the smallest path metric among every possible path to the destination. The metrics specify the delay status of each node's forwarding path to the destination and, therefore, indicate "good" forwarders. Considering the node metric given in **Proposition 1**, the candidate list is consequently proposed as follows.

Proposition 2 (For Step 2 of SMOR-1): For Source CR_S, the jth node in the candidate list is node i if $j = |V_i|$, where the set

$$V_x = \{k | k \in n \text{ and } m_k \leq m_x\}. \tag{31}$$

The candidate list prioritizes CR forwarders with respect to the node metric (i.e., m_i, $i \in n$). The triggering ratio and counter of relay enable opportunistic forwarding for SMOR-1. Specifically, the relay uses packet reception as a signal to transmit by advancing its counter with ratio. We propose ratio Φ_z for relay z as follows.

Proposition 3 (Triggering Ratio Φ_i for Node i): Let $j \bar{<} i$ denote node j having a smaller node metric than i. For relay node i, its triggering ratio is set as

$$\Phi_i = \frac{\Lambda_i}{\sum_{j \bar{>} i} \Lambda_j \vartheta_{ji}} \tag{32}$$

where ϑ_{ji} is equal to $c_{S_{ji}}$ in the slotted system and to $c_{DU_{ji}}$ or $c_{VU_{ji}}$ in the unslotted system. Λ_i, which is the expected number of transmissions that i must make to route one packet from the source to the destination, is obtained as

$$\Lambda_i = \frac{\sum_{j \bar{>} i} \left[\Lambda_j \vartheta_{ji} \prod_{k \bar{<} i} (1 - \vartheta_{ik})\right]}{1 - \prod_{k \bar{<} i} (1 - \vartheta_{ik})}. \tag{33}$$

Proof: ϑ_{ji} denotes the workable probability of opportunistic link ji. Considering that one packet transmits from the source to the destination, the number of packets that node i must forward is $\sum_{j \bar{>} i} [\Lambda_j \vartheta_{ji} \prod_{k \bar{<} i} (1 - \vartheta_{jk})]$ in expectation. Furthermore, for each forwarded packet, the number of transmissions that i makes is a geometric random variable with success probability $1 - \prod_{k \bar{<} i} (1 - \vartheta_{ik})$. Thus, we obtain Λ_i and end the proof. ■

Via multihop transmissions of SMOR-1, *Source*'s data packets traverse the whole network to *Destination*, avoiding interference to PSs by cooperative relay and, thus, fulfilling reliable communications in regular CRAHNs.

B. SMOR-2

To deal with networking in large-scale CRAHNs, we involve the concept of opportunistic routing with geographic routing and propose SMOR-2. Specifically, such scenarios happen when the network grows larger (a million nodes with spatial distribution), and local information alone is not suitable for reliable end-to-end routing anymore. Then, SMOR-2 exploits the global information (i.e., the direction from the source to the destination) for networking in such a large network. In the following, we assume *Source* knows the direction of *Destination* in a large-scale CRAHN.

Algorithm 2 (SMOR-2)

1) The *Source* first partitions its traffic into batches of packets for transmissions.
2) At each *Source*'s available time slot, *Source* makes its forwarder set (i.e., $i \in R(CR_S)$) by the *Destination*'s direction, requests workable probabilities from its forwarders (i.e., $\vartheta_{CR_S i}$, $i \in R(CR_S)$), and prioritizes forwarders in the forwarding candidate list with respect to link metric $m_{CR_S,i}$. *Source* then randomly mixes packets in a batch via random network coding [43] and broadcasts coded packet with the list and the availability information (i.e., $\vartheta_{CR_S i}, i \in R(CR_S)$).

3) While the ACK message is not heard from *Destination*,
   a) *Source* repeats Step 2 until it hears ACK.
   b) For each relay node z, if z receives a packet from others, it decodes the packet and recodes packet's incoming direction in θ_z, saves unheard information in its buffer, and checks the list.
      i) If z is in the list, z calculates its triggering ratio Φ_z according to the list and advances its counter by the ratio.
   c) At each z's available time slot, z examines whether its counter is positive.
      1) If so, z makes its forwarder set (i.e., $i \in R(z)$) from θ_z, requests $\nu^0_{z,i}$, and priorities forwarders in the new list according to $m_{z,i}$. z then randomly mixes its buffered packets, broadcasts coded packet with the new list and $\nu^0_{z,i}$ $(i \in R(z))$, and decrements its counter by one.
4) *Destination* continuously decodes the collection of coded packets to verify whether it gets all packets of the batch. If so, *Destination* broadcasts ACK back to *Source*, eliminating the packets buffered in relay machines and enabling the next transmission batch.

SMOR-2 utilizes link metrics and candidate lists in the delay perspective, extends the random concept of networks to geographic opportunistic routing, and thus fulfills the cooperative diversity in large-scale CRAHNs. To guide link transmissions along the direction from *Source* to *Destination*, forwarder selections for *Source* in Step 2 and for relay nodes in Step 3c1 are given in the following proposition.

Proposition 4: Given Destination CR_D's direction, the forwarder set of *Source* CR_S, which is denoted by $R(CR_S)$, is

$$R(CR_S) = \left\{ j | j \in N(CR_S) \text{ and } |\angle \overrightarrow{CR_S CR_D} - \angle \overrightarrow{CR_S j}| \le 90^\circ \right\} \quad (34)$$

where $N(i)$ is i's neighbors, and $\angle \vec{x}$ is the angle of vector $\vec{x}$; for relay z, when it receives a packet from i, θ_z is updated as

$$\theta_z \cap [\angle \overrightarrow{xz} - 90^\circ, \angle \overrightarrow{xz} + 90^\circ]. \quad (35)$$

If the intersection gives ϕ, θ_z is set to [0, 360°]. Furthermore, z's forwarder set, which is denoted by $R(z)$, is given as

$$R(z) = \left\{ j | j \in N(z) \text{ and } \angle \overrightarrow{Sj} \in \theta_z \right\}. \quad (36)$$

With the aid of **Proposition 4**, all packets are transmitted along the $\overrightarrow{CR_S CR_D}$ direction in multihop forwarding. In addition, to establish the candidate list for *Source* and relay nodes, the link metric on the direct transmission of *Source* and relay node z (i.e., $m_{CR_S,i}$ and $m_{z,i}$) are provided in **Proposition 5**.

Proposition 5 (Link Metric $m_{i,j}$ for $L_{i,j}$): For link $L_{i,j}$ between node i and node j, link metric $m_{i,j}$ is obtained as the opportunistic link delay.

It is noted that the required link delay of **Proposition 5** is given in **Lemma 4** and **Lemma 5**. Then, the forwarding candidate lists are proposed as follows.

Proposition 6 [For Step 2 and Step 3c1]: For Source CR_S, the jth node in CR_S's forwarding candidate list is machine i if $j = |V_i^{CR_S}|$, where the set

$$V_x^{CR_S} = \{k | k \in R(CR_S) \text{ and } m_{CR_S,k} \le m_{CR_S,x}\}. \quad (37)$$

For relay z receiving a packet from node y, the jth node in z's candidate list is i if $j = |V_i^z|$, where the set

$$V_x^z = \{k | k \in R(z)/y \text{ and } m_{z,k} \le m_{z,x}\}. \quad (38)$$

Proof: The candidate list prioritizes the machine's forwarders regarding the link metric (i.e., $m_{CR_S,i}$ and $m_{z,i}$). For relay z, z's list should not include that which transmits packet to z for avoiding invalid transmissions, and thus, we end the proof. ■

Similar to SMOR-1, a CR relay uses packet reception to indicate its forwarding by advancing its counter with the triggering ratio, and we propose ratio Φ_z for relay z as follows.

Proposition 7: For relay node z receiving a packet with the candidate list from node y, if z is the jth candidate of the list, z's triggering ratio is set as

$$\Phi_z = \prod_{k \lessdot z} (1 - \vartheta_{yk}) \quad (39)$$

where $i \lessdot j$ denotes that node i is preferred as y's forwarder than node j (i.e., $m_{y,i} < m_{y,z}$).

Proof: As a packet receiving from y, relay z should forward only when other relay(s), who have better forwarding qualities regarding the link metric, fail the reception from y. Φ_z gives the probability for that event and, thus, triggers z's forwarding. ■

By concatenating multiple opportunistic routings along the source–destination direction, SMOR-2 successfully provides dependable data transportation in large-scale CRAHNs.

VI. Performance Evaluation

We list all simulation parameters and values in Table II and evaluate SMOR-1 and SMOR-2 algorithms, respectively. The usages of both algorithms depend on the network size (or precisely the network models). When the network is small (i.e., only a few nodes or regular CRAHNs), SMOR-1 serves as a great feasible data transportation. However, when the network grows larger (a million nodes with spatial distribution) and local information is not enough for reliable end-to-end routing, SMOR-2 takes charge of packet delivery with the aid of global information (i.e., the direction from the source to the destination). To validate the SMOR-1 protocol, we deliberate it over a three-node relay network for variable packet size in a slotted system (i.e., the VS case). Through this simple but meaningful network topology, it clearly reveals the practicability of SMOR-1 over opportunistic fading links in regular CRAHNs and the advantage of opportunistic forwarding than a predetermined route strategy through further study in a wireless relay network. On the other hand, to validate the SMOR-2 protocol, we deploy the protocol with the per-node-based model over the Poisson network topology [41] for the VS case. Given the area and density settings for PS and CR in Table II, the Poisson network topology is established. We endorse the favor of SMOR-2 as a geographic opportunistic routing in large-scale CRAHNs and further evaluate the superiority of SMOR-2 over

TABLE II
PARAMETER SETTING FOR PERFORMANCE EVALUATION OVER REGULAR AND LARGE-SCALE CRAHNs

SMOR-1 with VS case in regular CRAHN		**SMOR-2 with per-node based model and VS case in large-scaled CRAHN**	
Parameter	*Value*	*Parameter*	*Value*
$n+1$	3	The Area for PPP [41]	36
σ_{SD}	$[0.1, 1]$ in CRAHN; 1 in wireless network	$\tilde{\lambda}_{ST}$	1
σ_{SR} and σ_{RD}	1	$\tilde{\lambda}_{PT}$	0.3 in CRAHN; 0 in wireless network
ν_{SD}	0.45	ψ	0.01 (dB)
ν_{SR} and ν_{RD}	0.97	P_{ST} and N_0	0.42 (dB)
λ	$[0, 9]$ (pkt/sec)	W_T	5×10^3 (Hz)
μ	200 (pkt/sec) in CRAHN; 50 (pkt/sec) in wireless network	α	3.5
		λ in Figure 6	5 (pkt/sec)

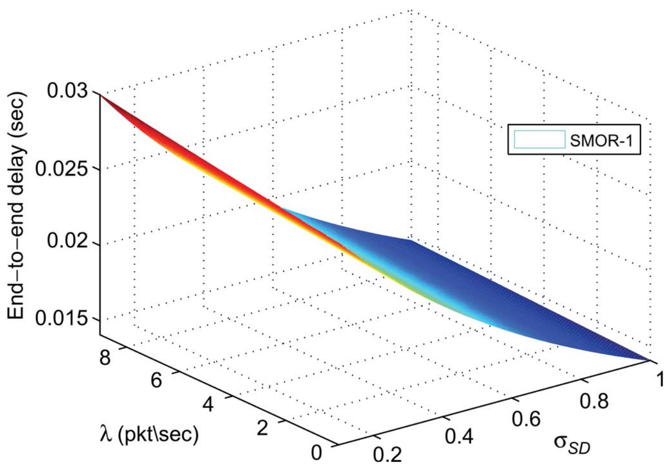

Fig. 4. End-to-end delay of SMOR-1 with respect to λ and σ_{SD} in a regular CRAHN.

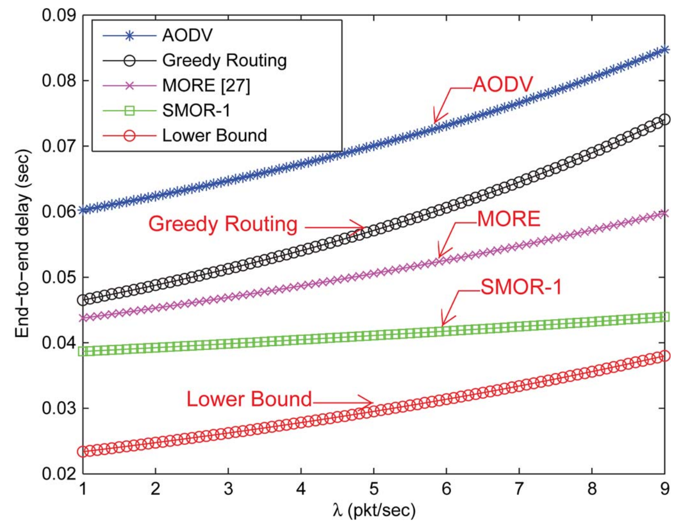

Fig. 5. Routing algorithms in a wireless network for single-packet source transmission.

prominent routing algorithms in a wireless Poisson network. Simulation results verify remarkable delay improvement over benchmarks in the literature due to SMOR-1 and SMOR-2 with respect to regular and large-scale CRAHNs, fulfilling reliable communications over CRAHNs.

A. Performance of SMOR-1 Protocol in Regular CRAHNs

SMOR-1 fulfills cooperative networking by the opportunistic routing concept in regular CRAHNs. The spectrum available probability (i.e., σ_{xy}) represents the opportunistic and dynamic spectrum availability and accounts for the spectrum usage of PS's traffic over the geographic area. To include the wireless fading effects, we further set the successful transmission rate (i.e., ν_{xy}) accounting for the distance between nodes x and y. Finally, CR's Poisson packet arrival rate (i.e., λ) and packet service rate of links (i.e., μ) are set for the avoidance of the whole network being crashed from traffic overload. As verified in Fig. 4, SMOR-1 has larger delay in low availability of direct link and with heavy traffic flow from CR_S. That is, SMOR-1 identifies good transmission quality for CRs through opportunistic nature of links and successfully provides a practically workable end-to-end transportation for regular CRAHN.

Moreover, to compare with state-of-the-art algorithms, we deploy SMOR-1 in wireless networks. σ_{SD}, σ_{SR}, and σ_{RD} are all set to 1 for SMOR-1 in a wireless relay network. We compare our protocol with MORE [27], which utilizes a heuristic-base solution with network coding and serves as the benchmark for opportunistic routing in wireless networks. In Fig. 5, different from other algorithms, SMOR-1 concerns a fading channel with a successful transmission rate (i.e., ν_{xy}) and allows cooperative relay with good transmitted capability to forward *Source*'s traffic. With increasingly incoming traffic flow, SMOR-1 achieves prominent improvement from its cooperative diversity and elaborates the routing mechanism against delay performance. It approves that SMOR-1 remarkably outperforms other algorithms.

B. Performance of SMOR-2 Protocol in Large-Scale CRAHNs

To exhibit the success of SMOR-2 with the further challenge of large-scale CRAHNs, we compare SMOR-2 with a greedy routing algorithm, which aims to route packets within the shortest path [44]. Under different opportunistic natures of the network characterized by activity of PS-Txs, Fig. 6 shows the better performance of SMOR-2 from its cooperative diversity gain with the aid of cooperative relays. Due to different available geographical information, Fig. 7 demonstrates SMOR-2's capability for large-scale networks. When the source–destination pair is far apart in a large area, the algorithm might not access the destination by just one time. In that case, SMOR-2 could localize forwarding with concatenation between each time. With $\tilde{\lambda}_{ST} = 1$ and $\tilde{\lambda}_{PT} = 0.3$, Fig. 7 shows different times of opportunistic routing needed for the algorithm. It also verifies

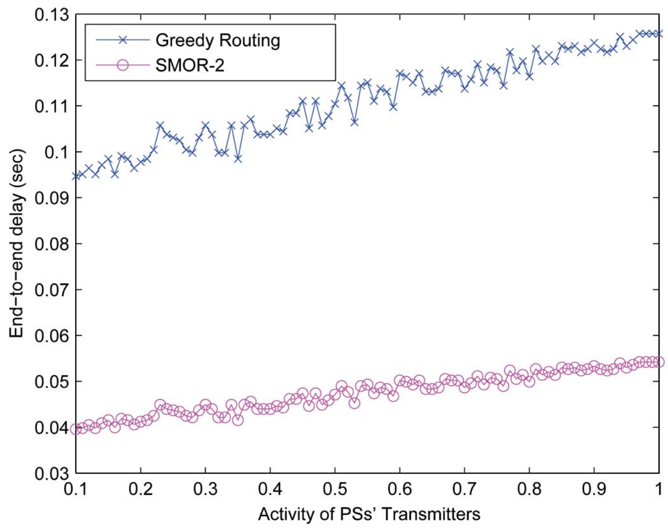

Fig. 6. End-to-end delay of SMOR-2 with respect to PS-Txs' activities.

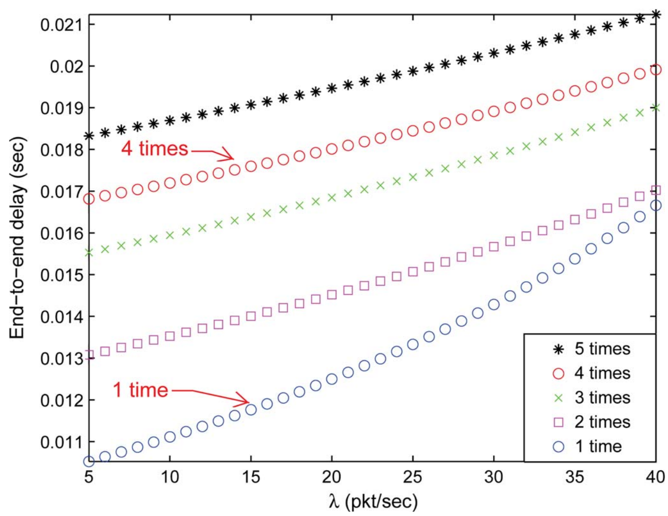

Fig. 7. Different times of opportunistic routing via SMOR-2 for end-to-end transmission.

that more available geographic information implies less operations of opportunistic routing and yields better performance of SMOR-2. To further evaluate the superiority of SMOR-2 over several prominent routing algorithms, we deploy SMOR-2 in a wireless Poisson network by setting $\tilde{\lambda}_{PT} = 0$. Fig. 8 shows that SMOR-2's performance approaches the lower bound better than others and suggests preferred cooperative in a Poisson network.

VII. Conclusion and Future Work

This paper has provided the complete analysis for transmission delay over underlay CRAHNs with wireless fading channels and proposed SMOR-1 and SMOR-2 algorithms to establish reliable end-to-end transportation. Cogitating the opportunistic nature, the spectrum map serves as an information aggregation platform to dynamically update all kinds of sensing and inference results for both algorithms. Aiming for regular CRAHNs, SMOR-1 set the orthogonal property between PSs' and CRs' spectrum usages in the spatial domain and perfectly protected PSs' traffic from interruption by CRs' transmission. On the other hand, SMOR-2 promoted spatial reuse in a given

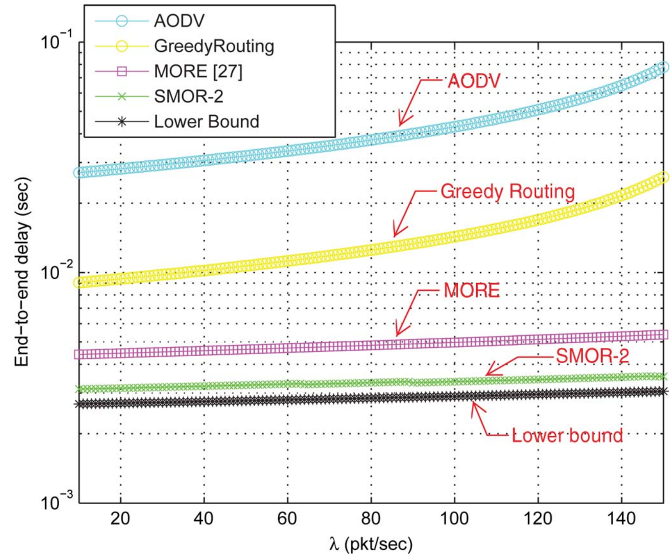

Fig. 8. Routing algorithms in a wireless Poisson network.

geographic area by enabling CR concurrent transmissions in large-scale CRAHNs. Simulations demonstrated remarkable performance due to network-coding-inspired cross-layer opportunistic routing with highly dynamic available opportunistic links.

With the feasible transportation over CRAHNs established by this paper, the possible future work is classified into three categories: upper layer control designs, physical information retrieval, and realistic implementation. First, while the workable routing algorithms are designed, there is still a need to guarantee the traffic QoS, such as network throughput. A possible research direction might be to study the relationship between end-to-end delay and throughput. Second, as we extract the physical transmission qualities from the spectrum map, such physical information can be further examined from a practical testbed. Practical implementation of the spectrum map might degrade our benchmark of network delay due to the inaccuracy of the map. Finally, the realistic implementation serves as the validation of our cross-layer design. Although such an issue is often a great challenge, our protocol-oriented design is independent of any practical module and, thus, enjoys great practicability in implementation. Therefore, this research certifies the feasibility of spectrum maps to serve spectrum-aware functions and facilitates a new paradigm for multihop transmissions in CRAHNs.

References

[1] "Unlicensed operation in the TV broadcast bands," Washington, DC, USA, ET Docket 08-260, Nov. 2008.

[2] J. Mitola and G. M. Jr., "Cognitive radio: Making software radios more personal," *IEEE Pers. Commun.*, vol. 6, no. 6, pp. 13–18, Aug. 1999.

[3] I. F. Akyildiz, W. Y. Lee, M. C. Vuran, and S. Mohanty, "NeXt generation/dynamic spectrum access/cognitive radio wireless networks: A survey," *Comput. Netw.*, vol. 50, no. 13, pp. 2127–2159, Sep. 2006.

[4] Y. C. Liang, K. C. Chen, J. Y. Li, and P. Mahonen, "Cognitive radio networking and communications: An overview," *IEEE Trans. Veh. Technol.*, vol. 60, no. 7, pp. 3386–3407, Sep. 2011.

[5] S. Sengupta and K. Subbalakshmi, "Open research issues in multi-hop cognitive radio networks," *IEEE Commun. Mag.*, vol. 51, no. 4, pp. 168–176, Apr. 2013.

[6] M. Cesana, F. Cuomo, and E. Ekici, “Routing in cognitive radio networks: Challenges and solutions,” *Ad Hoc Netw.*, vol. 9, no. 3, pp. 228–248, May 2011.
[7] A. Goldsmith, S. A. Jafar, I. Mari, and S. Srinivasa, “Breaking spectrum gridlock with cognitive radios: An information theoretic perspective,” *Proc. IEEE*, vol. 97, no. 5, pp. 894–914, May 2009.
[8] K. C. Chen, S. Y. Tu, and C. K. Yu, “Statistical inference in cognitive radio networks,” in *Proc. 4th ChinaCOM*, Aug. 2009, pp. 1–10.
[9] J. Wilson and N. Patwari, “Radio tomographic imaging with wireless networks,” *IEEE Trans. Mobile Comput.*, vol. 9, no. 5, pp. 621–632, May 2010.
[10] R. C. Qiu, Z. Hu, M. C. Wicks, S. J. Hou, L. Li, and J. L. Gray, “Wireless tomography, Part II: A system engineering approach,” in *Proc. 5th Int. Waveform Diversity Des. Conf.*, 2010, pp. 277–282.
[11] T. W. Chiang and K. C. Chen, “Synthetic aperture radar construction of spectrum map for cognitive radio networking,” in *Proc. 6th IWCMC*, 2010, pp. 631–635.
[12] S. Y. Shih and K. C. Chen, “Compressed sensing construction of spectrum map for routing in cognitive radio networks,” *Wireless Commun. Mobile Comput.*, vol. 12, no. 18, pp. 1592–1607, Dec. 2012.
[13] C. K. Yu and K. C. Chen, “Spectrum map retrieval by cognitive radio network tomography,” in *Proc. IEEE GLOBECOM Workshop*, Dec. 2011, pp. 986–991.
[14] K. C. Chen, S. Y. Tu, and C. K. Yu, “Statistical inference in cognitive radio networks,” in *Proc. ChinaCOM*, Aug. 2009, pp. 1–10.
[15] S. Geirhofer, L. Tong, and B. M. Sadler, “Dynamic spectrum access in the time domain: Modeling and exploiting white space,” *IEEE Commun. Mag.*, vol. 45, no. 5, pp. 66–72, May 2007.
[16] I. F. Akyildiz, W. Y. Lee, and K. R. Chowdhury, “CRAHNs: Cognitive radio ad hoc networks,” *Ad Hoc Netw.*, vol. 7, no. 5, pp. 810–836, Jul. 2009.
[17] Y. T. Hou, Y. Shi, and H. D. Sherali, “Spectrum sharing for multi-hop networking with cognitive radios,” *IEEE J. Sel. Areas Commun.*, vol. 26, no. 1, pp. 146–155, Jan. 2008.
[18] K. R. Chowdhury and M. D. Felice, “SEARCH: A routing protocol for mobile cogniive radio ad-hoc networks,” in *Proc. IEEE SARNOFF*, Mar. 2009, pp. 1–6.
[19] K. R. Chowdhury, M. D. Felice, and I. F. Akyildiz, “TCP CRAHN: A transport control protocol for cognitive radio ad hoc networks,” *IEEE Trans. Mobile Comput.*, vol. 12, no. 4, pp. 790–803, Apr. 2013.
[20] A. Abbagnale and F. Cuomo, “Gymkhana: A connectivity-based routing scheme for cognitive radio ad hoc networks,” in *Proc. IEEE INFOCOM*, 2010, pp. 1–5.
[21] S. Sharma, Y. Shi, Y. T. Hou, H. D. Sherali, and S. Kompella, “Cooperative communications in multi-hop wireless networks: Joint flow routing and relay node assignment,” in *Proc. IEEE INFOCOM*, Mar. 2010, pp. 1–9.
[22] Z. Feng and Y. Yang, “Throughput analysis of secondary networks in dynamic spectrum access networks,” in *Proc. IEEE INFOCOM Workshops*, Mar. 2010, pp. 1–6.
[23] T. Yazane, H. Masuyama, S. Kasahara, and Y. Takahashi, “End-to-end throughput analysis of multihop wireless networks with network coding,” in *Proc. IEEE ICC*, May 2010, pp. 1–5.
[24] S. Hua, H. Liu, M. Wu, and S. S. Panwar, “Exploiting MIMO antennas in cooperative cognitive radio networks,” in *Proc. IEEE INFOCOM*, Apr. 2011, pp. 2714–2722.
[25] S. Y. Lien, S. M. Cheng, S. Y. Shih, and K. C. Chen, “Radio resource management for QoS guarantees in cyber-physical systems,” *IEEE Trans. Parallel Distrib. Syst.*, vol. 23, no. 9, pp. 1752–1761, Sep. 2012.
[26] W. Cedric, “Opportunistic routing in dynamic ad hoc networks: The OPRAH protocol,” in *Proc. IEEE MASS*, Oct. 2006, pp. 570–573.
[27] S. Chachulski, M. Jennings, S. Katti, and D. Katabi, “Trading structure for randomness in wireless opportunistic routing,” in *Proc. SIGCOMM Conf. Appl., Technol., Architect., Protocols Comput. Commun.*, Aug. 2007, pp. 169–180.
[28] R. Zheng and C. Li, “How good is opportunistic routing?—A reality check under Rayleigh fading channels,” in *Proc. 11th Int. Symp. MSWiM*, Oct. 2008, pp. 260–267.
[29] H. Khalifé, N. Malouch, and S. Fdida, “Multihop cognitive radio networks: To route or not to route,” *IEEE Netw.*, vol. 23, no. 4, pp. 20–25, Jul./Aug. 2009.
[30] B. Mumey, J. Tang, I. Judson, and D. Stevens, “On routing and channel selection in cognitive radio mesh networks,” *IEEE Trans. Veh. Technol.*, vol. 61, no. 9, pp. 4118–4128, Nov. 2012.
[31] A. Cacciapuoti, I. Akyildiz, and L. Paura, “Correlation-aware user selection for cooperative spectrum sensing in cognitive radio ad hoc networks,” *IEEE J. Sel. Areas Commun.*, vol. 30, no. 2, pp. 297–306, Feb. 2012.
[32] S. C. Lin and K. C. Chen, “Spectrum aware opportunistic routing in cognitive radio networks,” in *Proc. IEEE GLOBECOM*, Dec. 2010, pp. 1–6.
[33] C. K. Yu, K. C. Chen, and S. M. Cheng, “Cognitive radio network tomography,” *IEEE Trans. Veh. Technol.*, vol. 59, no. 4, pp. 1980–1997, May 2010.
[34] A. Goldsmith, *Wireless Communications*. Cambridge, U.K.: Cambridge Univ. Press, 2005.
[35] D. Tse and P. Viswanath, *Fundamentals of Wireless Communication*. Cambridge, U.K.: Cambridge Univ. Press, 2005.
[36] D. Gross, J. F. Shortle, and C. M. Harris, *Fundamentals of Queueing Theory*, 4th ed. Hoboken, NJ, USA: Wiley, 2008.
[37] S. Karlin and H. M. Taylor, *A First Course in Stochastic Processes*. New York, NY, USA: Academic, 1975.
[38] M. Xie and M. Haenggi, “Towards an end-to-end delay analysis of wireless multihop networks,” *Ad Hoc Netw.*, vol. 7, no. 5, pp. 849–861, Jul. 2009.
[39] M. Haenggi, J. G. Andrews, F. Baccelli, O. Dousse, and M. Franceschetti, “Stochastic geometry and random graphs for the analysis and design of wireless networks,” *IEEE J. Sel. Areas Commun.*, vol. 27, no. 7, pp. 1029–1046, Sep. 2009.
[40] P. Gupta and P. R. Kumar, “Capacity of wireless networks,” *IEEE Trans. Inf. Theory*, vol. 46, no. 2, pp. 388–404, Mar. 2000.
[41] D. Stoyan, W. S. Kendall, and J. Mecke, *Stochastic Geometry and Its Applications*, 2nd ed. New York, NY, USA: Wiley, 1995.
[42] Y. Lin, X. Zhang, and B. Li, “CodeOR: Opportunistic routing in wireless mesh networks with segmented network coding,” in *Proc. IEEE ICNP*, 2008, pp. 13–22.
[43] T. Ho, M. Médard, J. Shi, M. Effros, and D. R. Karger, “On randomized network coding,” in *Proc. 41st Annu. Allerton Conf. Commun., Control, Comput.*, Oct. 2003, pp. 1–10.
[44] D. Bertsekas and R. Gallager, *Data Networks*. Upper Saddle River, NJ, USA: Prentice-Hall, 1987.

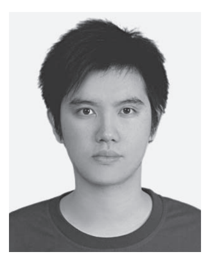

Shih-Chun Lin (S’12) received the B.S. degree in electrical engineering and the M.S. degree in communication engineering from National Taiwan University, Taipei, Taiwan, in 2008 and 2010, respectively. He is currently pursuing the Ph.D. degree with the School of Electrical and Computer Engineering, Georgia Institute of Technology, Atlanta, GA, USA.

His research interests include large-scale sensor networks, dynamic spectrum access, and statistical scheduling in wireless systems.

Kwang-Cheng Chen (M’89–SM’93–F’07) received the B.S. degree from National Taiwan University, Taipei, Taiwan, in 1983 and the M.S. and Ph.D. degrees from the University of Maryland, College Park, MD, USA, in 1987 and 1989, respectively, all in electrical engineering.

From 1987 to 1998, he was with SSE, COMSAT, IBM Thomas J. Watson Research Center, Ossining, NY, USA, and National Tsing Hua University, Hsinchu, Taiwan, in mobile communications and networks. Since 1998, he has been with National Taiwan University, where he is a Distinguished Professor and the Associate Dean in academic affairs of the College of Electrical Engineering and Computer Science. He has authored and co-authored over 250 technical papers. He is the holder of more than 20 U.S. patents. He co-edited (with R. DeMarca) the book *Mobile WiMAX* (Wiley, 2008), authored the book *Principles of Communications* (River, 2009), and co-authored (with R. Prasad) the book *Cognitive Radio Networks* (Wiley, 2009). His research interests include wireless communications and network science.

Dr. Chen has been actively involved in the organization of various IEEE conferences as the General/Technical Program Committee Chair/Co-Chair. He has served on the editorial board of a few IEEE journals and many international journals and has served in various positions within the IEEE. He also actively participates in and has contributed essential technology to various IEEE 802, Bluetooth, and 3GPP wireless standards. He has received a number of awards, including the 2011 IEEE COMSOC WTC Recognition Award, and has co-authored a few award-winning papers published in IEEE ComSoc journals and conferences.